

Encoded error calibration for a coded aperture spectrometer based on deconvolution

MING-BO CHI,^{1,2} YI-HUI WU,^{1,*} DAN-DAN GE,^{1,2} WEN-CHAO ZHOU,¹ PENG HAO,¹ AND YONG-SHUN LIU¹

¹State Key Laboratory of Applied Optics, Changchun Institute of Optics, Fine Mechanics and Physics, Chinese Academy of Sciences, Changchun 130033, China

²University of Chinese Academy of Sciences, Beijing 100039, China

*Corresponding author: yihuiwu@ciomp.ac.cn

Received 30 November 2015; revised 18 January 2016; accepted 18 January 2016; posted 19 January 2016 (Doc. ID 254831); published 19 February 2016

The principle of a 2D coded aperture spectrometer is described in this paper. The crosstalk of adjacent rows, which is caused by the optical system's point-spread function and the nonuniform illumination of the apertures, is the main source of the system decoded errors. Through the analysis of the effect of the crosstalk and nonuniform illumination on the decoded spectrum, the encoding matrix is modified. Based on the new encoding equation, an algorithm using Gold's deconvolution method is proposed to remove the crosstalk of adjacent rows. In the end, we evaluate the effect of this method through a series of contrast experiments. © 2016 Optical Society of America

OCIS codes: (120.6200) Spectrometers and spectroscopic instrumentation; (300.6190) Spectrometers; (100.1830) Deconvolution.

<http://dx.doi.org/10.1364/AO.55.001500>

1. INTRODUCTION

In a traditional single-slit spectrometer, shift images of the entrance slit are generated by the optics and dispersive elements at the detector plane by wavelength. However, the narrow slit, which can enhance the spectrometer resolution, results in a loss of light, which reduces the signal-to-noise ratio (SNR) of the spectrometer [1]. In order to balance this trade-off, a coded aperture spectrometer, which uses the Hadamard transform, was designed and constructed. An encoding mask with a coded slit array functions together with an image CCD to realize multichannel encoding of the incident light instead of the traditional single slit, which will bring about a higher SNR and a reasonable spectra resolution at the same time [2–4].

Because of the point-spread function (PSF) and nonuniform illumination, the optical system cannot implement the encoding process perfectly, which will lead to system errors in the decoded spectrum. The encoding process of the coded aperture spectrometer can be seen as a series of compound measurements of all the spectral channels. In theory, these compound measurements should be independent of each other. However, affected by the optical system's PSF in the direction perpendicular to the diffusion direction, the encoded signal generated by one row of the slit array will be widened and will multiply with the signal generated by adjacent rows. If this crosstalk is ignored, there will be system errors in the decoded spectrum. So there were completely opaque rows of one CCD pixel height placed between each row in the code in the traditional design [5]. These dead rows were used to reduce the crosstalk between

adjacent codes of the slit array. Unfortunately, the dead rows will cause a large waste of CCD pixels and then decrease the SNR enhancement ratio. The SNR enhancement ratio is proportional to the order of the encoding matrix or the number of compound measurements [3]. A larger order means a larger number of the dead rows, which will decrease the SNR enhancement ratio in turn. When using the mask with opaque rows, a much larger CCD is needed to realize a proper SNR enhancement ratio, which will be an obstacle to the practicality of this spectrometer.

The foundation of the encoding process is that apertures in the same column or same channel generate the same spectrum on the detector. When using a fiber to transmit the incident light from a diffuse source, the illumination on the apertures is nonuniform. The traditional solution is using an engineered diffuser. But the diffuser will cause a loss of light and make the mechanics of the spectrometer more complex. What is more, even with the help of the diffuser, the illumination cannot be absolutely uniform.

In this paper, we propose a signal-processing method to deal with these system errors. First, we analyze how the crosstalk and nonuniform illumination affect the encoding process of this spectrometer, and use a modified encoding equation to describe the real encoding process. Then we propose the calibration method based on the deconvolution and modified encoding matrix. In Section 3, we describe the details of contrast experiments to experimentally verify the effectiveness of this method. Furthermore, this method can also be useful in compressive

coded aperture spectral imaging, which also uses coded apertures [6,7].

2. THEORETICAL ANALYSIS

A. Principle of the Coded Aperture Spectrometer

The encoding and decoding process of the coded aperture spectrometer is shown in Fig. 1. The coded apertures we used are encoded in an $N * N$ binary matrix, which usually utilizes a Hadamard S matrix [8]. Ignoring the effect of optical distortion and other system errors, the apertures in the same column generate the same spectral distribution on the detector plane as they have the same location along the dispersion direction of the spectrometer. In other words, they belong to the same spectra-detecting channel. The spectra signal generated by the apertures in the same row multiplies on the same pixel of the detector and this can be seen as a compound measurement of these spectra channels. In each measurement, the code “1” means that the corresponding channel is included and code “0” means not. With the results of N compound measurements, we can get a spectrum with a higher SNR and reasonable spectra resolution after decoding and other signal-processing processes. The sets of spectra channels can be represented by a vector, ψ , the encoding matrix is denoted by S , and the results of the compound measurements are denoted by η . Thus, the encoding process corresponds to the matrix equation as follows:

$$\eta = S\psi. \tag{1}$$

If we use S^{-1} to denote the inverse of S , then the decoding equation can be shown as follows:

$$\psi = S^{-1}\eta. \tag{2}$$

Then we can get the decoded spectra of all the spectral channels. Any of the two decoded spectra are the same, except a wavelength shift caused by the distance between the two columns of apertures in the diffusion direction. After the calibration of the wavelength shift, we can multiply all the decoded spectra to get a much larger SNR enhancement.

B. Calibration of System Errors Caused by the Crosstalk between Adjacent Rows of Apertures

The encoded signals of every two rows of the coded aperture should be independent of each other. However, affected by the PSF of the optical system in the direction perpendicular to the

diffusion direction, the encoded signal of one row of the coded apertures will be widened and spread into the signals of its adjacent rows. If we use $\Delta\eta$ to denote the crosstalk and ψ' to denote the decoded spectrum affected by the crosstalk, then the real decoding equation can be described as follows:

$$\psi' = S^{-1}\eta + S^{-1}\Delta\eta'. \tag{3}$$

As the crosstalk $\Delta\eta'$ is not encoded in matrix S , we cannot get the correct decoded spectrum by just using the theoretical decoding Eq. (2) with the existence of the decoded error $S^{-1}\Delta\eta$.

Figure 2(a) is a schematic of the crosstalk between adjacent compound measurements on one column of detector pixels. As shown in Fig. 2(a), the encoded signal of one compound measurement ($\eta_1, \eta_2, \text{ or } \eta_3$) spreads into adjacent rows and multiplies with the signal of the other compound measurements, which will cause an overlap. The encoded data we practically get ($\eta'_1, \eta'_2, \eta'_3$) are blurred by the crosstalk. If ($\eta'_1, \eta'_2, \eta'_3$) is directly used in the decoding Eq. (2), there will be system decoded errors in the decoded spectrum as shown by Eq. (3). Figure 2(b) shows how the opaque rows between two rows of coded apertures weaken the influence of the crosstalk. With the opaque rows placed between every two rows of coded apertures, most of the crosstalk will spread into the detector pixels corresponding to the opaque rows. So the encoded data we practically get are nearly proportional to the original correctly encoded data.

However, as we can see from Fig. 2(b), the pixels corresponding to the opaque rows are wasted and the encoding area will become larger, which means a larger detector is needed whereas the order of the encoding matrix remains the same. In other words, the order of the encoding matrix should decrease because of the design of the opaque rows when functioning together with a CCD with proper size. If the imaging CCD has m rows of pixels and the subaperture corresponds to only one row of pixels, then the maximum order of the encoding matrix is m . For a large m , the theoretical SNR gain brought about by the Hadamard transform is as follows [3]:

$$G_H = \frac{\sqrt{m}}{2}. \tag{4}$$

If the opaque rows of one pixel height are placed between every two rows of subapertures, then the maximum order of the encoding matrix we can realize is near $m/2$. If we describe G'_H as the Hadamard transform SNR gain using this coded apertures, then we get

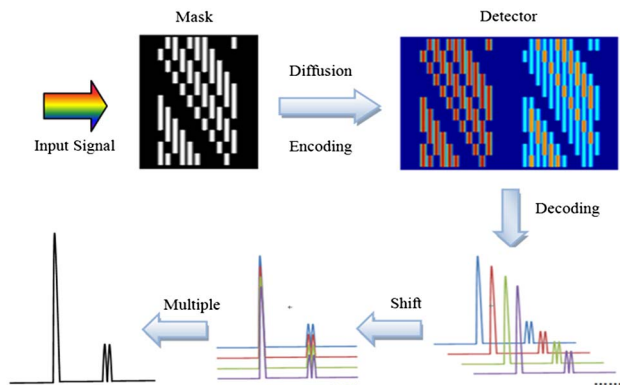


Fig. 1. Encoding and decoding principle of the coded aperture spectrometer.

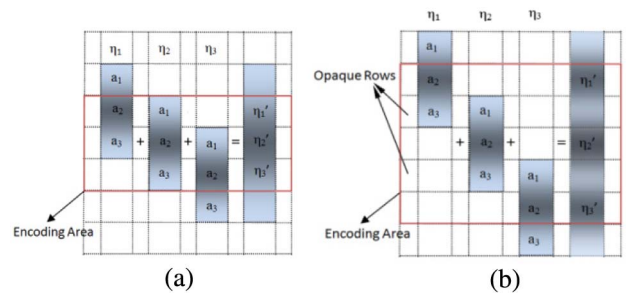


Fig. 2. (a) Schematic of the crosstalk caused by the PSF of the optical system. (b) The schematic of the signal distribution when the opaque rows are placed between the coded apertures.

$$\frac{G'_H}{G_H} = \frac{\sqrt{2}}{2}. \quad (5)$$

Then we can see that if the opaque rows are used to weaken the crosstalk, then the order of the encoding matrix we can realize with a proper CCD will be seriously decreased and this will cause a loss of the SNR gain. However, if we do not use the opaque rows and directly implement the decoding algorithm on the row data, then there will be decoded errors in the decoded spectrum. So a new method is needed because of this trade-off.

The minimum unit in the encoding and decoding process of the coded aperture spectrometer is the subaperture, whose size is an integer times pixels and much larger than the wavelength of the incident light. The optical system of this spectrometer is a noncoherent imaging system. For the example shown in Fig. 2, we just use $(a_1, a_2, a_3)^T$ to represent the discrete distribution of one subaperture's image on the detector in the direction perpendicular to the diffusion direction. The sample interval is equal to the height of the subaperture. In this paper, this distribution is called the subaperture spread function, which in fact is the convolution of the height function of the subaperture and the PSF of the optical system. When using coded apertures without the opaque rows as shown in Fig. 2(a), a_2 is the influence coefficient of one measurement's impact on itself, whereas a_1 and a_3 are the influence coefficients of this measurement's impact on its adjacent two measurements. The other influence coefficients are assumed to be 0 to simplify the analysis. If the impact of the optical system's aberration is ignored, then this distribution is nearly space constant. So the crosstalk between the compound measurements can be expressed mathematically as follows:

$$\begin{bmatrix} a_2 & a_1 & 0 \\ a_3 & a_2 & a_1 \\ 0 & a_3 & a_2 \end{bmatrix} \begin{bmatrix} \eta_1 \\ \eta_2 \\ \eta_3 \end{bmatrix} = \begin{bmatrix} \eta'_1 \\ \eta'_2 \\ \eta'_3 \end{bmatrix}. \quad (6)$$

If the distorting matrix constructed by $(a_1, a_2, a_3)^T$ in Eq. (4) is denoted by P , then Eq. (6) can be written as

$$\eta' = P\eta, \quad (7)$$

and then we can get the ideal encoded data η through the following equation where P^{-1} represents the inverse of the matrix P :

$$\eta = P^{-1}\eta'. \quad (8)$$

According to Eq. (2), the practical decoding equation considering the effect of the crosstalk should be described as

$$\psi = S^{-1}P^{-1}\eta'. \quad (9)$$

As shown in Eq. (6), if the subaperture spread function is used as the convolution kernel, then the encoded data affected by the crosstalk can be seen as the convolution of the ideal encoded data and the subaperture spread function. Equation (8) is the simplest deconvolution process, which may be affected badly by the random noise in the original data of the measurements. A stable deconvolution method is needed and we choose the Gold iterative algorithm because its solution is positive [9,10]. Because the subaperture spread function is the convolution of the subaperture's height function and the optical system's PSF, it follows a Gauss distribution. Thus, the coefficient

a_2 is usually much larger than the other coefficients and all the coefficients are positive. So the distorting matrix P is symmetric and has diagonal dominance, which can be easily derived from Eq. (6). Therefore, P is nonsingular and it satisfies the convergence condition of the Gold iterative algorithm of deconvolution. Then we should use this algorithm on the raw data to remove the effect of the crosstalk before the decoding process with the measurement of the subaperture spread function; otherwise there will be system errors in the decoded spectrum.

C. Calibration of the System Errors Caused by Nonuniform Illumination

If the coded apertures are directly illuminated by the diffuse source, then the light falling on the apertures will differ from each other. This will break the foundation of the coded aperture spectrometer in that the apertures in the same column generate the same distribution. For example, when using a 3×3 cyclic S matrix as the encoding matrix, light of different wavelengths ($\lambda_1, \lambda_2, \lambda_3$) from three channels overlap on the same column of detector pixels. The intensities of the three channels are denoted by ϕ_{λ_1} , ϕ_{λ_2} , and ϕ_{λ_3} , respectively. Given that the intensity deviation caused by the nonuniform illumination only exists in the first channel, the practical encoding process can be represented by a modified matrix as shown in Eq. (10) where η'_1 , η'_2 , and η'_3 represent the measurement result on the detector:

$$\begin{bmatrix} \eta'_1 \\ \eta'_2 \\ \eta'_3 \end{bmatrix} = \begin{bmatrix} 1 + \varepsilon_1 & 1 & 0 \\ 1 + \varepsilon_2 & 0 & 1 \\ 0 & 1 & 1 \end{bmatrix} \begin{bmatrix} \phi_{\lambda_1} \\ \phi_{\lambda_2} \\ \phi_{\lambda_3} \end{bmatrix}. \quad (10)$$

If we ignore the effect of the nonuniform illumination and use the ideal binary encoding matrix in the decoding process, then the system decoded errors shown in Eq. (11) will arise:

$$\begin{cases} \delta_{\phi_{\lambda_1}} = \frac{1}{2}(\varepsilon_1 + \varepsilon_2)\phi_{\lambda_1} \\ \delta_{\phi_{\lambda_2}} = \frac{1}{2}(\varepsilon_1 - \varepsilon_2)\phi_{\lambda_1} \\ \delta_{\phi_{\lambda_3}} = \frac{1}{2}(\varepsilon_2 - \varepsilon_1)\phi_{\lambda_1} \end{cases}. \quad (11)$$

As we can see from the above equation, the decoded spectra of channels 2 and 3 will be affected by channel 1, which has nonuniform illumination. The larger the degree of the nonuniform illumination ($\varepsilon_1 - \varepsilon_2$) and the intensity of channel 1 at wavelength λ_1 , the larger the decoded errors of channels 2 and 3. So the detection of a light source with discrete spectrum will be badly affected by the nonuniform illumination because the spectral intensity of the source changes a lot with wavelength in the peak region and there are huge differences between the intensities of the spectral channels on the same detector pixel. For example, when the spectral region of channel 2 or 3 whose intensity is near 0 multiplies with the peak region of channel 1, it can be easily derived from Eq. (11) that there will be a nonexistent peak in this region of the decoded spectrum of channel 2 or 3 in the detection of an Hg lamp.

So to avoid this system error, a measurement of ε_1 and ε_2 should be made to modify the encoding matrix S . Using a source with a discrete spectrum such as an Hg lamp, we can measure the intensity of each of the apertures at the same wavelength, which is proportional to the whole intensity of the corresponding aperture. Take the ratio of the intensity of one slit

and the largest intensity in the same column or the same channel to replace the corresponding code “1” in the ideal encoding matrix. This means that only a part of the spectra signal of this channel is taken into the corresponding compound measurement. If the modified encoding matrix is denoted by S_m , then the real encoding process can be expressed as follows:

$$\eta = PS_m\psi. \tag{12}$$

Thus, in order to remove the system errors caused by the PSF and nonuniform illumination, the modified decoding equation can be described by Eq. (13):

$$\psi = S_m^{-1}P^{-1}\eta. \tag{13}$$

3. EXPERIMENTS AND ANALYSIS

Figure 3 illustrates the experimental setup of the coded aperture spectrometer. The optical system of the spectrometer is the same as that of a traditional single-slit spectrometer, except for the coded apertures. The incident light from the light source transmits through the coded apertures and is collimated by a collimating mirror. The collimated light is subsequently dispersed by a grating and imaged on an imaging detector by a condensing mirror. The CCD detector translates the encoded light signal into a digital signal and transmits it to a computer for the decoding process.

As shown in Fig. 4, we manufactured two kinds of masks with coded apertures curved on them to perform contrast experiments with the help of MEMS technology. The two masks have the same order of coded apertures ($N = 19$), but one of them is designed without the opaque rows and the other has opaque rows. On both the masks, one row of coded apertures corresponds to two rows of CCD pixels. The opaque row between two adjacent rows takes one row of CCD pixels. When functioning with the coded apertures with opaque rows, the imaging CCD should have 57 rows of pixels at least, and it is 50% more than the size of the CCD needed when functioning with the coded apertures without the opaque rows, which only needs 38 rows of pixels.

In order to implement Gold’s deconvolution algorithm, we must first construct the convolution kernel or the subaperture spread function. We replaced the coded apertures of the spectrometer with a single slit that has the same size as the subaperture in the coded apertures. Then we use the spectrometer to detect a light source that has a discrete spectrum with sharp peaks, for example, an Hg lamp or a laser. Through the slit

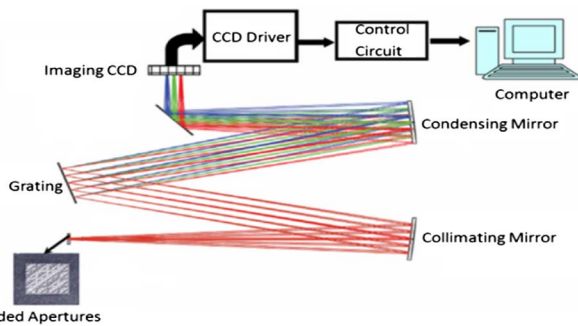


Fig. 3. Schematic of the coded aperture spectrometer.

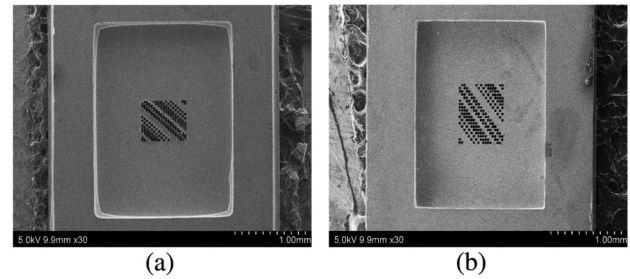


Fig. 4. (a) Coded apertures without opaque rows. (b) The coded apertures with opaque rows.

image on the CCD, we can get the intensity distribution of one subaperture in the direction perpendicular to the diffusion direction and then we can get the influence coefficient we needed.

We have detected the spectrum of the Hg lamp using the two kinds of coded apertures shown in Fig. 4. First, we used the coded apertures that use the opaque rows to weaken the effect of the crosstalk, and the decoded spectrum is shown in Fig. 5(a). The full width at half-maximum (FWHM) of the peaks is 1.5 nm. Then we just changed the encoding mask to the coded apertures without the opaque rows, whereas the other settings of the spectrometer remained the same. Affected by the crosstalk, the FWHM of the peaks of the spectrum, which is directly decoded from the data without any signal processing, is 1.8 nm. As we can see from Fig. 5(b), the peak at 577 nm could be hardly distinguished from the peak at 579 nm. After removing the crosstalk with the method we

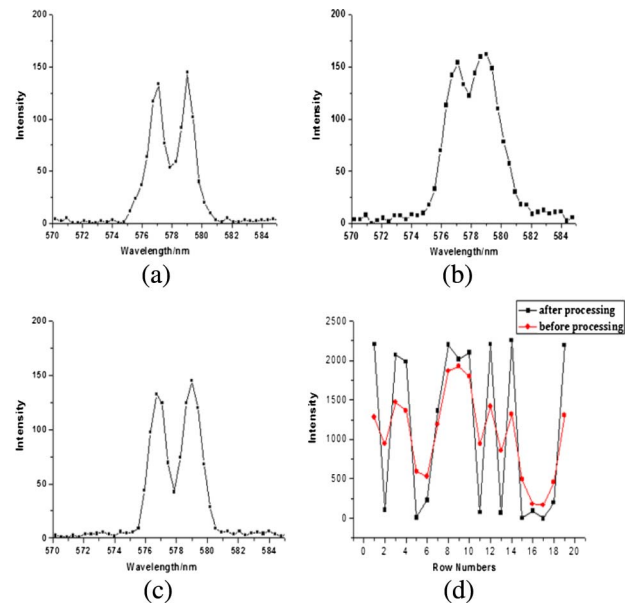


Fig. 5. (a) Decoded spectrum of the Hg lamp using the opaque rows to remove the crosstalk. (b) The spectrum decoded directly from the data without any processing when using the coded apertures without the opaque rows. (c) The decoded spectrum using the algorithm based on deconvolution to remove the crosstalk. (d) The encoded data of one column of pixels before and after removing the crosstalk when using the coded apertures without opaque rows.

proposed, the FWHM of the decoded peak is 1.4 nm. In Fig. 5(c), the peaks can be well distinguished from each other. The resolution of the spectrometer that we constructed has improved nearly 25% with the help of the method we proposed, which is a little better than that of the decoded spectrum using the opaque rows to remove the crosstalk.

Through the contrast of Figs. 5(b) and 5(c), we can find that the crosstalk caused by the PSF will widen the FWHM of the decoded spectrum when ignoring the crosstalk in the decoding process. The results of one group of compound measurements before and after removing the crosstalk when using the coded apertures without opaque rows are shown in Fig. 5(d). In the Hg lamp spectrum, the spectral intensity changes rapidly with wavelength in the spectral region that contains a sharp peak and the spectra of different encoding channels have a wavelength shift between each other as shown in Fig. 1. In one group of the compound measurements in this region, the intensity of one channel may be very large whereas the intensity of the other channels may be near 0. As shown in Fig. 5(d), the intensities of the compound measurements that only include weak spectral channels are near 0 and increase with adjacent measurements through the crosstalk. Then it can be concluded that the decoded intensities of the weak spectral channels are increased and the decoded intensity of the intense spectral channel is decreased. In other words, in the decoded spectra of all the spectral channels, for example, the intensity at the weak spectral regions of channel A is increased, affected by the peak region of channel B through the crosstalk; the decoded intensity at the weak spectral regions beside the peak of channel B is also increased in the same way. This will lead to the fact that the FWHM of the decoded spectrum of one spectral channel will be widened, as its peak intensity will decrease and the decoded intensity at the region around the peak increases. That also means that the resolution of the decoded spectrum will decrease because of the crosstalk that is caused by the optical system's PSF in the direction perpendicular to the diffusion direction.

We have measured the intensity of the peak at 546 nm in the decoded Hg lamp spectra 30 times, using the signal-processing algorithm based on deconvolution and opaque rows to remove the crosstalk. The two measurements are made using the same light source, optical system, detector, and integration time. The only difference lies in the encoding mask. The results are shown in Fig. 6. To evaluate the quality of the two measurements, we compute the SNR of the decoded spectra, which is defined as the ratio of the mean and standard deviation of the measured peak intensity. For the decoded spectrum that used the algorithm based on deconvolution, the mean and SNR of the measured intensity at 546 nm are 1428.6 and 549.5, respectively. When using the coded apertures with the opaque rows, the mean and SNR are 858.4 and 357.7, respectively.

From the above experiment results, we can find that the resolution and SNR of the decoded spectrum using the algorithm based on deconvolution are better than those of the decoded spectrum that uses the opaque rows to remove the crosstalk. In the design of the coded apertures with the opaque rows, the opaque rows only take one row of pixels to make full use of the CCD as much as possible. The adjacent rows of the coded aperture could still affect each other through crosstalk, although the

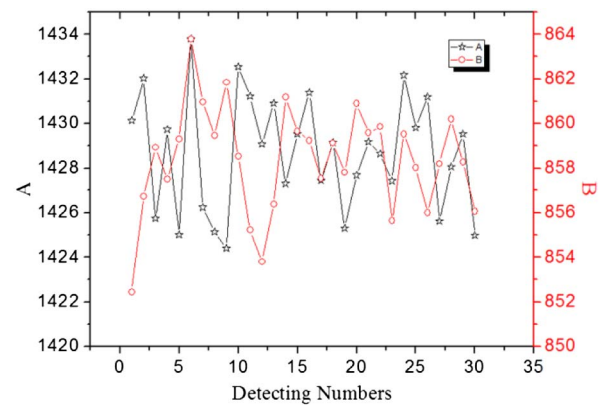


Fig. 6. (a) Measured intensity of the peak at 546 nm in the decoded Hg lamp spectrum that used the signal-processing algorithm to remove the crosstalk. (b) Measured intensity of the peak at 546 nm in the decoded Hg lamp spectrum that used the opaque rows.

opaque rows can remove most of the effect of the crosstalk. But when using the signal-processing algorithm, the influences of one row of coded apertures on the other rows are all taken into consideration. On the other hand, when using the coded apertures with the opaque rows, only part of the incident light was actually used in the compound measurements. When using the algorithm based on deconvolution, the light signal spread into adjacent rows was taken back to its source and used in the encoding and decoding process. Thus, the decoded intensity of the spectrum using the algorithm is much higher than that of the spectrum that used the opaque row. This will still lead to an increase of the SNR, although the standard deviation of the decoded intensities using the signal processing is a little larger. In one word, the calibration effect of the algorithm based on deconvolution is better than the effect when using the opaque rows, besides the need of a smaller CCD.

We used the coded apertures without the opaque rows to detect the spectrum of a deuterium lamp, which is continuous and also has a sharp peak at 656 nm. The spectra directly decoded from the raw data and the calibrated spectrum, which gets rid of the influence of the crosstalk based on the algorithm we proposed, are shown in Fig. 7(a). In the previous experiment, we have proved that the algorithm we proposed has a very good effect on the removal of the decoded error caused by the crosstalk. Therefore, we use the difference between the two decoded spectra to make an approximate estimate of the decoded errors caused by the crosstalk as shown in Fig. 7(b). By comparing Figs. 7(a) and 7(b), it can be derived that the decoded error caused by the crosstalk is dependent on the type of the spectrum. The decoded errors in the wave band of 600–650 nm, in which the spectral intensity changes little with wavelength, are near 0, whereas there are large decoded errors in the band near the spectral line at 656 nm, in which the spectral intensity changes a lot with wavelength.

In one group of compound measurements, the wavelengths of the spectral channels are different and belong to a small wave band whose width is proportional to the order of the encoding matrix or the number of spectral channels. If the spectrum is nearly flat and smooth in this band, then the intensities of the

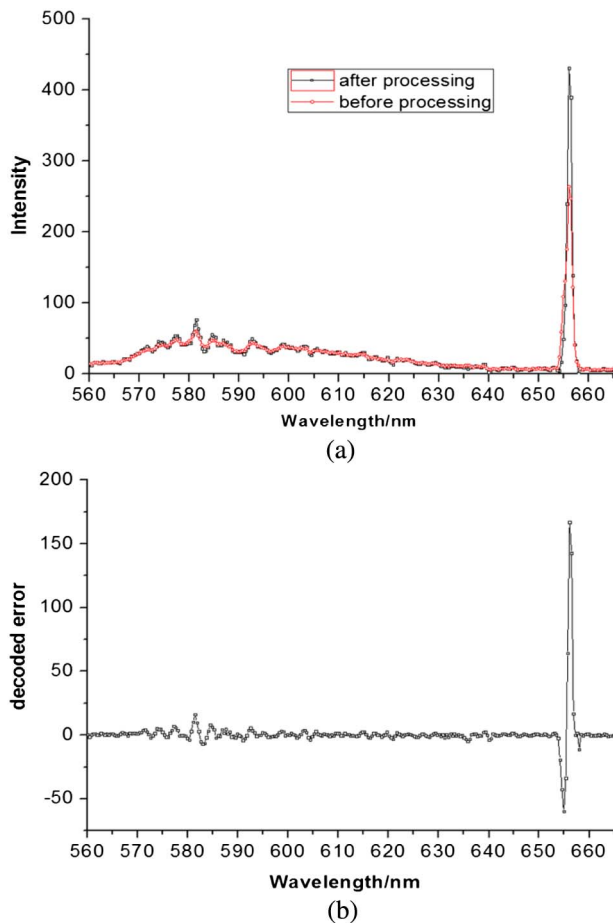


Fig. 7. (a) Decoded spectra of the deuterium lamp before and after removing the effect of the crosstalk with the algorithm we proposed. (b) The difference between the two decoded spectra.

spectral channels are almost the same. As each compound measurement includes the same number of spectral channels, the intensity of one compound measurement has no significant variation from that of another. The energy that transforms from one measurement to adjacent measurements through the crosstalk is nearly equal to the energy it gets from the others. In this case, the crosstalk has little effect on the decoded spectrum. On the contrary, the spectral intensity will change greatly with wavelength in the case where there is a sharp spectral line in this band. So the intensities of the compound measurements in this band may differ a lot from each other and the measurement with low intensity will be affected badly by the measurement with high intensity through the crosstalk, which will lead to a large decoded error.

Having removed the crosstalk, there are still some intensity differences between the compound measurements as shown in Fig. 5(d). These differences are mainly caused by the nonuniform illumination. Figure 8 illustrates the spectra decoded with the unmodified encoding matrix and the modified matrix. The intensity of the spectral region beside the peak at 546 nm in the Hg lamp spectrum should be near 0. However, affected by the nonuniform illumination, there are nonexistent peaks besides the peak at 546 nm in the spectrum decoded using

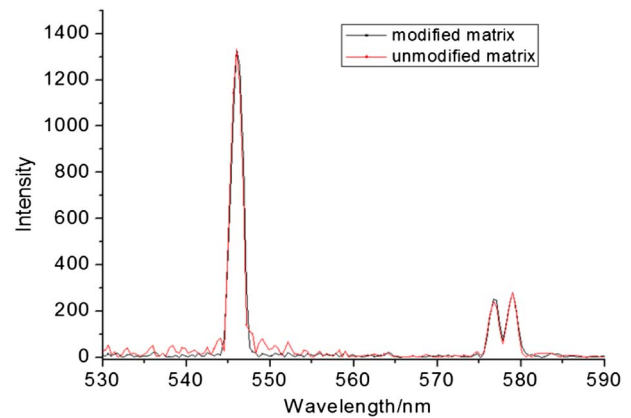


Fig. 8. Normalized spectra decoded using the unmodified matrix and modified matrix after removing the crosstalk.

the unmodified encoding matrix, which is consistent with the previous analysis in Section 2.C. The maximum decoded error in the region beside 546 nm is near 10% of the decoded intensity at 546 nm. The impact of the nonuniform illumination on the region beside the peaks at 577 and 579 nm is not as significant as that on the region beside the peak at 546 nm because the spectral signal at 577 or 579 nm is much weaker than that at 546 nm. Then we acquired the encoded images of the Hg lamp at 546 nm 30 times to modify the encoding matrix in the way we proposed in this paper. Decoded with this modified matrix, the ratio of the largest decoded error in the region beside 546 nm and the peak intensity at 546 nm is less than 2% as shown in Fig. 8.

4. DISCUSSION

Equation (13) describes the practical decoded process of the coded aperture spectrometer to remove the system decoded errors caused by the crosstalk and nonuniform illumination. The crosstalk removal algorithm based on the Gold deconvolution method should first be implemented on the raw data, and then the decoding algorithm should be implemented using the matrix modified by the measurement of the nonuniformity of the illumination. The modification of the encoding matrix to calibrate the nonuniform illumination and the usage of the diffuser are not in conflict. The modified matrix can be used as a supplement to the diffuser because the diffuser cannot make the illumination on the apertures absolutely uniform. With the help of the removal algorithm of the crosstalk proposed in this paper, the resolution of the coded aperture spectrometer we constructed has improved nearly 25%, which is higher than that in the method using the opaque rows as well as the SNR. Furthermore, this method will not cause a waste of the CCD pixels, which has great significance for practical application of the coded aperture spectrometer.

Based on the detection of the deuterium lamp's spectrum, we made a qualitative analysis of the relationship between the decoded errors caused by the crosstalk and the types of spectra. When the spectral intensity varies significantly with wavelength, there will be large decoded errors caused by the crosstalk

in this band. However, if the spectral intensity changes little in some wave band, there is almost no decoded error caused by the crosstalk. Furthermore, the width of the wave band included in one group of compound measurements is proportional to the order of the encoding matrix or the spectral channels.

Funding. The National High Technology Research and Development Program of China (2015AA042402).

REFERENCES

1. R. Riesenberger, A. Wuttig, G. Nitzsche, and B. Harnisch, "Optical MEMS for high-end micro-spectrometers," *Proc. SPIE* **4928**, 6–14 (2002).
2. R. A. Deverse, R. M. Hammaker, and W. G. Fateley, "Realization of the Hadamard multiplex advantage using a programmable optical mask in a dispersive flat-field," *Appl. Spectrosc.* **54**, 1751–1758 (2000).
3. G. Nitzsche and R. Riesenberger, "Noise, fluctuation and HADAMARD-transform-spectrometry," *Proc. SPIE* **5111**, 273–282 (2003).
4. M. E. Gehm, S. T. McCain, N. P. Pltsianis, D. J. Brady, and P. Potuluri, "Static two-dimensional aperture coding for multimodal, multiplex spectroscopy," *Appl. Opt.* **45**, 2965–3183 (2006).
5. A. A. Wagadarikar, M. E. Gehm, and D. J. Brady, "Performance comparison of aperture codes for multimodal, multiplex spectroscopy," *Appl. Opt.* **46**, 4932–4942 (2007).
6. A. Wagadarikar, R. John, R. Willett, and D. Brady, "Single disperser design for coded aperture snapshot spectral imaging," *Appl. Opt.* **47**, B44–B51 (2008).
7. G. R. Arce, D. J. Brady, L. Carin, H. Arguello, and D. S. Kittle, "Compressive coded aperture spectral imaging," *IEEE Signal Process. Mag.* **31**(1), 105–115 (2014).
8. M. Harwit and N. Sloane, *Hadamard Transform Optics* (Academic, 1979), pp. 200–228.
9. P. A. Jansson, *Deconvolution of Images and Spectra* (Dover, 2012), pp. 67–80.
10. P. Bandžuch, M. Morháč, and J. Krištiak, "Study of the Van Cittert and Gold iterative methods of deconvolution and their application in the deconvolution of experimental spectra of positron annihilation," *Nucl. Instrum. Methods Phys. Res. A* **384**, 506–515 (1997).